Austin Journal of Biosensors & Bioelectronics

Open Access

Austin Publishing Group

Research Article

Nanosensors of Fluorescent Carbon Quantum Dots Derived from Banana Peel: Application in Sr^{2+} and Co^{2+} Detection

Kaffash M[1], Bakhtparvar A[1], Rezvani-Noghani A[1], Hosseini S[2], Mokaberi P[1] and Chamani J[1]*

[1]Department of Biology, Faculty of Sciences, Mashhad Branch, Islamic Azad University, Mashhad, Iran

[2]Cancer Research center, Mashhad University of Medical Sciences, Mashhad, Iran

***Corresponding author:** Jamshidkhan Chamani, Department of Biology, Faculty of Sciences, Mashhad Branch, Islamic Azad University, Mashhad, Iran

Received: October 20, 2022; **Accepted:** November 19, 2022; **Published:** November 26, 2022

Abstract

Natural Carbon Quantum Dots (NCQDs) are known to contain photo luminescence property and stand as a promising nanomaterial group. Therefore, we intended to generate an intelligible and effective hydrothermal procedure for performing the green synthesis of this material through the usage of banana peel waste as a feasible and durable natural carbon source. The obtained NCQDs were characterized by the means of UV-visible absorption spectroscopy, spectrofluorometry, Fourier Transform Infrared Spectroscopy (FT-IR), X-Ray Diffraction (XRD), zeta potential, Atomic Force Microscopy (AFM), Field Emission Scanning Electron Microscopy (FE-SEM), Transmission Electron Microscopy (TEM), and Thermo Gravimetric Analysis (TGA). The lack of utilizing any toxic substances has guaranteed the safety of this procedure in all the biological practices. Therefore, the high crystalline and spherical morphology of synthesized NCQDS with an average roughness of about 5.9 nm were indicated by the results of TEM and XRD. We also observed a high water stability and solubility due to the presence of hydroxyl and carboxyl group and excitation- dependent emission performance with the satisfying quantum yield of 12 %. The zeta potential of prepared NCQDs reached up to -27.4 mV. Furthermore, in order to determine the low toxicity and favorable biocompatibility of this product, we studied the toxic effects of NCQDs on the fibroblast cell line of a normal mouse through the MTT assay. In conformity with the gathered data, these NCQDs contain the potential of being utilized as a nontoxic carrier and a fine alternative for bio-sensor, bio-imaging, and drug delivery applications. The development of these NCQDs was completed with the objective of acting as a highly sensitive fluorescent "on-off-on" switch sensor in the course of the selective and simultaneous sensing of Sr^{2+} and Co^{2+}. Fluorescence data revealed that the binding constants of Sr^{2+} and Co^{2+} to NCQDs were to be $1.39 \times 10^4\ M^{-1}$ and $1.58 \times 10^4\ M^{-1}$ respectively. The observations were indicative of a linear relationship among the Sr^{2+} and Co^{2+} ions volume and the fluorescence intensity throughout the range of 0 to 0.1 mM.

Keywords: CQDs; Banana peel; Hydrothermal; Spectroscopy; FESEM; MTT assay; Sensor

Introduction

Being the most proponent fluorescent nanoparticles, the application of Semiconductor quantum dots can be vastly detected as nanoprobe throughout the fields of sensing and bio-imaging due to containing distinctive optical qualities [16,26]. In spite of this fact, the concern for the toxicity of this substance to the health of humans and environment, caused by the existing heavy metal constituents in its structure, is gradually increasing [8]. The very first signs of carbon quantum dots discovery was reported in 2004 in the course of purifying single-walled carbon nano-tubes by the means of preparative electrophoresis [51]. Standing as a new category of fluorescent small carbon nanoparticles, Semiconductor quantum dots were considered as a replacement for carbon quantum dots due to containing an ultrafine smaller size, biocompatibility, super hydrophobicity, excellent photo luminescent properties, low cytotoxicity, and high chemical reliability [2,31]. The NCQDs can be applicable for substituting semiconductor QDs and organic fluorescent dyes for science applications.In addition, considering their certain features, this product can be applied in several applications of various areas such as bio-imaging, sensing, photo catalysis, drug delivery, cancer therapy, and etc [11,12,22,27,33,40,46,48,50,52,53,]. There are two principal methods in general for synthesizing NCQDs that include top-down and bottom-up routes. The cases of top-down methods for synthesizing CQDs involve the usage of different bases such as graphite, carbon fibers, coal, soot and biomass, which are performed through schematic treatments including arc-discharge, laser ablation, electrochemical oxidation, chemical oxidation, ultrasonic treatment, and solvothermal procedures [10,13,15,20,25,29,39,44,47]. On the other hand, the bottom-up approaches involve the synthesis of NCQDs by the exertion of precursors similar to folicacid, gelation, citric acid, and organic sources that include potato, grapefruit, watermelon, peanut shells, and pineapple [19,23,30,38,41]. The benefits of exerting plants for the fabrication of nano-particles

Citation: Kaffash M, Bakhtparvar A, Rezvani-Noghani A, Hosseini S, Mokaberi P and Chamani J. Nanosensors of Fluorescent Carbon Quantum Dots Derived from Banana Peel: Application in Sr^{2+} and Co^{2+} Detection. Austin J Biosens & Bioelectron. 2022; 7(1): 1041.

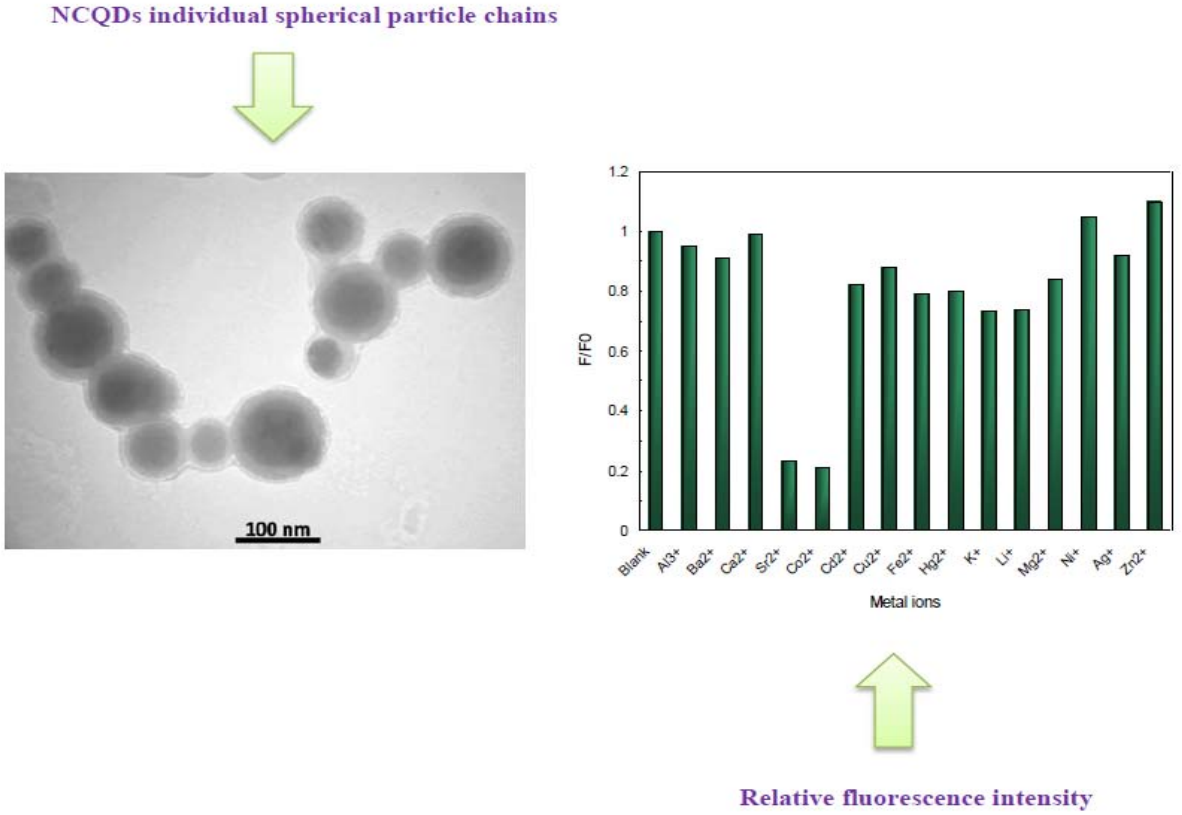

Mini-Abstract: The transmission electron microscope images of the prepared NCQDs and its individual spherical particle chains, scale bar indicates 100 nm along with relative fluorescence intensity of NCQDs in the presence of various metal ions.

have become evident by recent reports, which include their simple availability, safe handling, and being biodegradable. Furthermore, the usage of these waste sources for synthesizing purposes results in the reduction of pollution and also helps in cleaning up the environment from these waste materials [39,45]. Apparently, the fluorescence functionality of NCQDs can be improved through a more enhanced doping of hetero-atoms into the carbonaceous framework and surface passivation and furthermore, more qualified CQDs can be obtained facilely through the concurrent proceeding of hetero element doping and passivation [1,23]. Due to accommodating multifarious hetero-atoms, the simple synthesis of CQDs by natural substances results in the production of products that contain varying surface groups along with distinctive features without performing any passivation or modification. Consequently, many investigations have attempted to succeed in synthesizing CQDs by the usage of different natural biomass/bio-waste [6,32]. In bottom-up approaches, the synthesis of CQDs is performed through microwave irradiation, hydrothermal-solvothermal treatment, hydrothermal method, and plasma [9,36,41]. Standing as the most effective and facile technique, hydrothermal method functions on water system and can provide simple manipulation, un expensive apparatus, and fine selectivity on water system [43]. This method has been exerted by many researchers such as Arumugam Selva Sharma and co-workers, which performed the synthesis of CQDs and achieved a size of 2-4 nm by the usage of soy milk. Also, Sun and co-workers reported the synthesis of CQDs from selenicerusgr and if lours through the hydrothermal method while lacking the exertion of any additional oxidizing agents such as ethanol [4,43]. In this work, an uncomplicated, cheap, and applicable procedure for performing the synthesis of NCQDs by the usage of banana peel through green and facile hydrothermal method is introduced, which lacks the requirement of any chemical materials and was followed by characterizing the obtained product using different analytical techniques. The resulted NCQDs possess bright fluorescence and satisfying stability, as well as a quantum yield of 7.5 %. The results of Raman spectroscopy (D/G ratio of 0.85) indicated the purity of our synthesized NCQDs, while this fluorescent product was observed to contain a spherical shape with the average diameter of 5.9±0.14 nm. Considering their physicochemical features, the high potent of NCQDs as a promising product for mass scale manufacturing, bio-sensor, bio-imaging, and other biological implementations is undeniable.

Material and Methods

Materials

Banana was purchased from a local market in Mashhad, Iran. Sodium hydrogen carbonate and EDTA were obtained from Merck chemicals. All solvents were analytical grade and used without further purification. Millipore was used throughout the study.

Preparation of NCQDs

These biocompatible NCQDs were synthesized from banana peel waste via an innovative method, first we gathered some banana

peels and dried them in the sunlight, 3gr of obtained brown powder were added into 100 ml deionized water. This suspension was boiled and stirred at 70°C for 2h. After 2h, the upper liquid of the obtained solution were transferred into Teflon lined stainless steel autoclave. The autoclave was tightly sealed then placed into the oven at 150°C for 4h. Then, it had cooled to room temperature, the upper liquid were centrifuged at 8317.6 rcf (8000 rpm. min) for 10 minutes. Next, the obtained liquid passed through filter paper and the obtained light liquid were filtered with 0.22m filter to remove the large substances. For dispersing of the synthesized NCQDs, was done for 30 minutes. The obtained liquid was natural carbon quantum dot solution. A part of NCQDs was kept for UV-visible and PL spectra and the other part of liquid was dialyzed (MW=35 kD) for about 24h (Figure 1).

Powder of NCQDs for characterization: A part of NCQDs solution was taken out and vacuum freeze-dried (Freez dryer, operon, Korea, 1500W) for 24 h at -70°C to produce solid brown powder. The powdered samples were then stored at ambient temperature for further characterization.

Characterization

The obtained NCQDs from banana peel through hydrothermal method were characterized by various methods that conclude spectroscopic and microscopic techniques.

X-ray diffraction (XRD): The obtain information of particle sizer; crystallinity and phase purity of the synthesized NCQDs were analyzed by using X-ray diffraction (XRD) analysis. X-ray diffraction pattern was observed by using panalytical instrument (XPertoPro-Holland). X-ray pattern equipped with Cu K radiation (wavelength λ= 1.54 Å) with the targeted voltage of 40 kV and current of 30 mÅ. We were used Scherrer's equation

$$D = \frac{0.9\lambda}{\beta \frac{1}{2}\cos\theta}$$

to calculated average crystal size (D_{hkl}). D_{hkl} is about the crystallite dimensions of the diffracting planes of the miller that functions as an indicator for hkl, λ demonstrate the radiation wavelength (λ = 1.5406 Å), θ represents the diffraction angle, K is the correction factor (0.9), and $\beta_{1/2}$ stands for the peak width at the half maximum height (FWHM).

FTIR spectroscopy: The Fourier Transform Infrared Spectroscopy (FTIR, Thermo-Nicolet, Avatar 370, U) to analysis the functional groups of the samples in the spectral range of 400-4000 cm^{-1} and at a spectral resolution of 4 cm^{-1}at room temperature has been utilized. Due to the development of c-dots by the partial oxidation of a carbon precursor, carboxyl or carboxylic acid groups, hydroxyl groups and other/ epoxy are abundant on the surface of c-dots and so far the investigation of these groups containing oxygen, FTIR is a useful device.

DLS and Zeta potential: The Zeta Potential and DLS of the samples have been measured through the usage Zetasizer Nano S90, Malvern Instruments, (Malvern, UK) at room temperature. The sample of NCQDs was distilled water that had been utilized as the dispersant to avoid the effects of multiple scattering. We were used DLS methods for determine the size of these synthesized samples and also were used zeta potential for determining the electrical charges on the surface of nanoparticles and stability in water.

FESEM: The surface morphologies and the size of NCQDs have been assessed through the employment of FESEM by (TESCAN MIRA 3, Czech Republic).This process is being coated by gold with the magnification of 70.0 kx and at the accelerating voltage of 20 kV.

EDAX: Importance elements of the synthesized NCQDs such as carbon, oxygen, nitrogen have been measured by the usage of Energy Dispersive X-rays Spectroscopy (SAMX, Germany) at an accelerating voltage of 15 kV.

TEM: The morphological features and particle size of sample in order to understand information regarding shape, size and dispersion were investigated with a Zeiss (EM10C, Germany) transmission electron microscope (TEM) operating at 100 kV. These images were prepared as follows: The dilute aqueous solution of the sample was sonicated for 15 min (Misonix-S3000). Then, a portion of sample (20 µL) was dropped onto formvar carbon film on copper grid 300 mesh (EMS-USA) and dried thoroughly at room temperature.

AFM: To analyze the surface topography and also size of the obtained NCQDs, AFM imaging was performed by using Atomic force microscope (Brisk model).The powder of sample NCQDs was diluted in pure water and the designated samples have been sonicated for 5 min and these has been positioned on a glass slide and dried under room temperature.

Thermogravimetric analysis: We have used thermogravimetric analyzer (TGA-50, Shimadzu, Japan) to characterize the thermal stability of the involved samples, which had been carried out in air atmosphere and at a heating rate of 10 °C/min that started from 20°C and reached up to 560 °C. The weight loss of samples as a function of the temperature has been indicated on TG curve. The Derivative Thermogravimetric (DTG) curve has been utilized for the aim of highlighting the district of temperature in which each phenomenon has occurred.

UV-Visible spectroscopy: The UV-visible absorption spectrum of NCQDs was measured by the usage spectrophotometer V-630 (JASCO, Japan).The sample was diluted in pure water. The UV measurements were performed in the absorption wavelength of 200 to 800 nm at room temperature.

Spectrofluorometer: The fluorescent spectrum was evaluated with single beam fluorescence spectroscopy F-2500 (Hitachi, Japan) at room temperature. The obtained sample was diluted in pure water. The diluted sample was carried out in different excitation wavelength. (λ_{em}= 300, 320, 340, 360, 380, 400, 420 and 440 nm)

Quantum yield determination of NCQDs: The quantum yield (QY) of synthesized NCQDs was measured through the following equation:

$$\varphi_{x} = \varphi_{std}(I_{x}/A_{x})(A_{std}/I_{std})(\eta^{2}_{x}/\eta^{2}_{std}) \quad (1)$$

Where φx is the fluorescence quantum yield; x represents the samples, std is the reference compound. Quinine sulfate dissolved in 0.1 M H_{2SO4} (φ_{std} = 0.54) was chosen as the reference. η is the refractive index (1.33 for aqueous solution). A is the absorbance at the excitation wavelength. I, is the integrated fluorescence intensity under the fluorescence emission spectrum. In order to minimize re-absorption effects, the optical absorbency values were below 0.1 at the

excitation wavelength.

Cytotoxicity Assessment Method

The ability of certain chemicals or mediator cells to destroy living cells is known as cytotoxicity. In vitro cytotoxicity studies of the synthesized NCQDs from banana peel waste was performed on mouse normal fibroblast cell line by MTT assay to determine the biocompatibility and the suitability of the prepared NCQDs. Mitochondrial enzymes in live cells reduce soluble, yellow 3-(4, 5-dimethythiazol2-yl)-2, 5-diphenyl tetrazolium bromide (MTT) to an insoluble, purple formasan product. This insoluble product which have been cultured in Dulbecco's Modified Medium (DMEM) and incubated at a temperature of 37°C and 5% CO_2 is then dissolved in a solvent and measured to evaluate the viability of fibroblast cells. In order, the cell viability assay the fibroblast cells has been seeded onto 96-wells plates (ELISA), which accommodated a density of 10,000 cells per well, and have been allowed to adhere overnight. Subsequently, after shifting the medium and they had incubated (37°C in 5% CO_2) for the duration of 24 h the cells have been allowed to face the intensifying concentrations of NCQDs. A blank (DMEM without cells) and a positive control sample (DMEM with cells) have been evaluated as well, while every single treatment has been analyzed in quadruplicate. We have substituted the spent medium with 100 µl of fresh medium and thus, have appended 10 µl of MTT solution (5 mg/ ml PBS, sterile) to each well while incubating them for a period of 4h (37 °C, 5% CO_2); this process resulted in the fabrication of purple formazan crystals. As the next step, the prepared crystals have been dissolved through the addition of 100 µl of DMSO to each well subsequent to conveying the medium. The enzymatic reduction of yellow tetrazolium MTT to purple formasan has been measured by the application of a Synergy™ HT Multi-mode Microplate Reader (Biotek Instruments, Winooski, VT, USA) at 570 nm. The percentage of cell viability has been calculated through the utilization of Eq. 2.

$$\text{Cell viability} = \frac{A\ \text{exp-}\ A\ ctrl}{A\ pos - A\ ctrl} \qquad (2)$$

Where A_{exp} is related to the absorbance of NCQDs experiment (NCQDs + cell), A control would be the absorbance of the blank sample (Dulbecco's Modified Eagle's Medium (DMEM) without cells), and A positive demonstrate the absorbance of positive control (DMEM + cells).

Result and Discussion

Physicochemical Analysis of Natural Carbon Quantum Dots

XRD pattern: The crystalline structure, average crystallite size and purity of as-prepared nanoparticles were determined by XRD which are shown in (Figure 2). The XRD analysis of NCQDs demonstrated the well-defined, wide and major peaks centered at 28.42(002) and 40.71(101) also low density diffraction peak at 18.38 (002) which illustrating amorphous carbon phase and presence of graphite carbon [21,34]. Furthermore, the Average crystallite size was estimated 22 nm with Scherer formula.

FTIR spectroscopy: The functional group and surface structure of obtained NCQDs and banana peel have been analyzed through the usage of FTIR spectroscopy in (Figure 3). The characterized absorption bands at 3417.12 cm^{-1} attributed to large number of hydroxyl group residues (–OH) [3]. The stretching vibration band of 2926.11 $cm^{-1}$was mainly due to aliphatic C–H stretching vibrations in methylene groups present in banana peel [35]. The stretching vibration band of at 1699.43 cm^{-1} that represent the presence of carboxylic acid and other oxygen containing functional group [3]. The peaks around 1609.03, 1078.32, 1254.03, and 1395.89 cm^{-1} corresponded to the respective functional groups stretching vibration band of C=C, C-O-C, C-N, C-N-C, respectively that indicate the presence of oxygen and nitrogen element in/on the surface of NCQDs [5,7]. The presence of these functional groups on the NCQDs surface is responsible for their excellent dispersion in aqueous media [37]. Moreover, the peak at 780.02 cm^{-1} was identified of vibration -C-H in the synthesized NCQDs. The difference between the FTIR graphs of NCQDS and banana peel can be mentioned these peaks which were disappeared in NCQDs, the peaks of stretching =CH3 (2851.16 cm^{-}

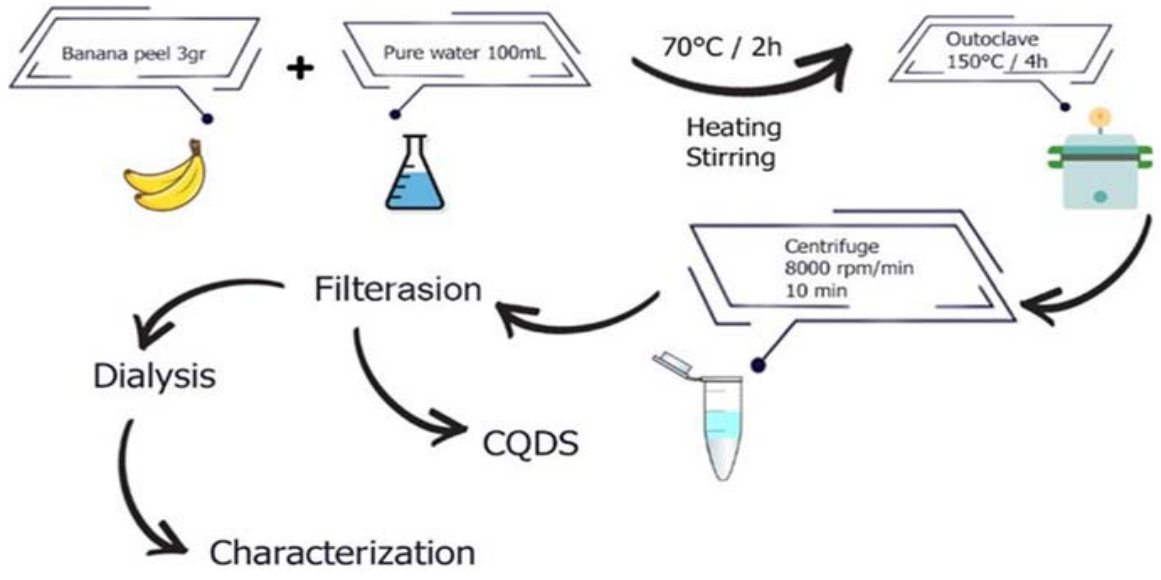

Figure 1: Schematic illustration of the formation of fluorescent NCQDs from banana peel waste via hydrothermal treatment.

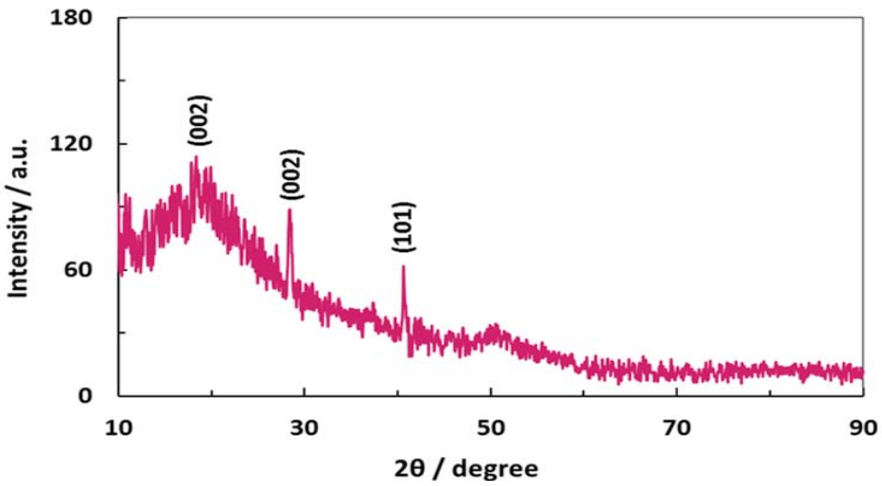

Figure 2: XRD pattern for the powder of obtained NCQDs at 2θ= 18.38, 28.42 and 40.71.

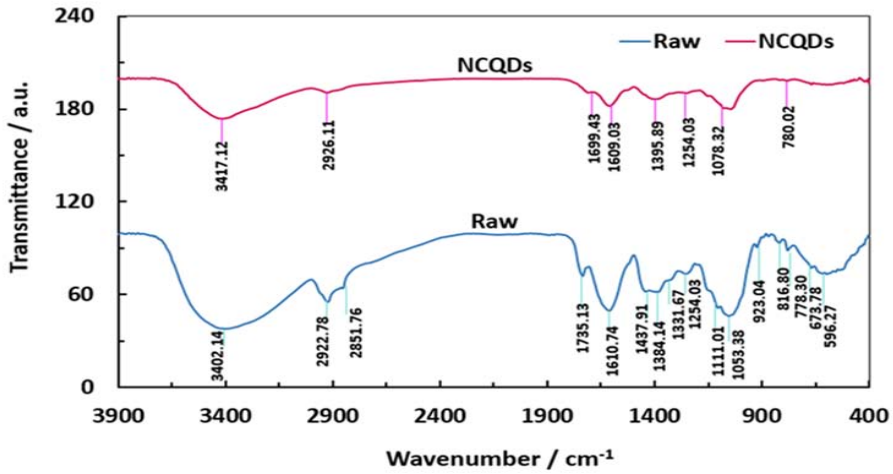

Figure 3: FTIR spectra of Raw sample (blue-a) and as prepared NCQDs (red-b).

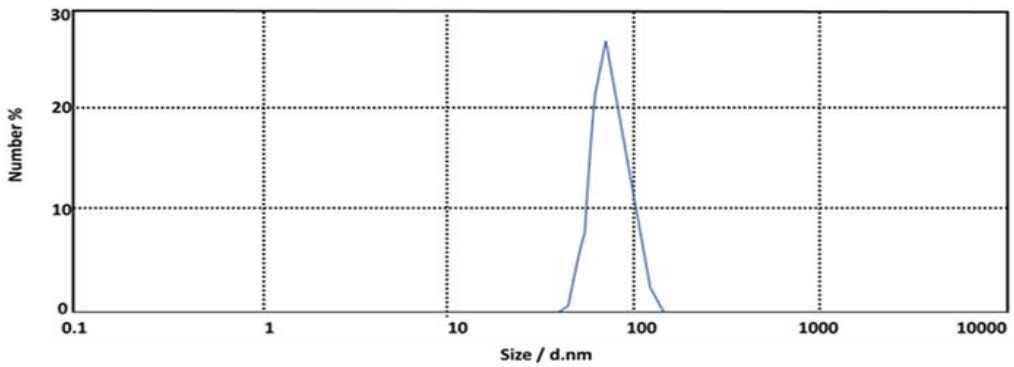

Figure 4: DLS measurement for aqueous solution of as-synthesized NCQDs.

^{1}), N-H (673.80 cm^{-1}), -CH-H (816.80 cm^{-1}), O-H (923.04 cm^{-1}), C-N (1254.03 cm^{-1}) and O-H (1331.67 cm^{-1}).

Structural Analysis of NCQDs

DLS and Zeta potential analysis: DLS analysis is a commonly method to survey the hydrodynamic diameter in colloidal solution which is shown in (Figure 4). The results indicate that the NCQDs are about 70 nm in size, which may be due to the agglomeration of the particles. Zeta potential analysis of NCQDs was employed to characterize the surface charge and stability of the synthesized

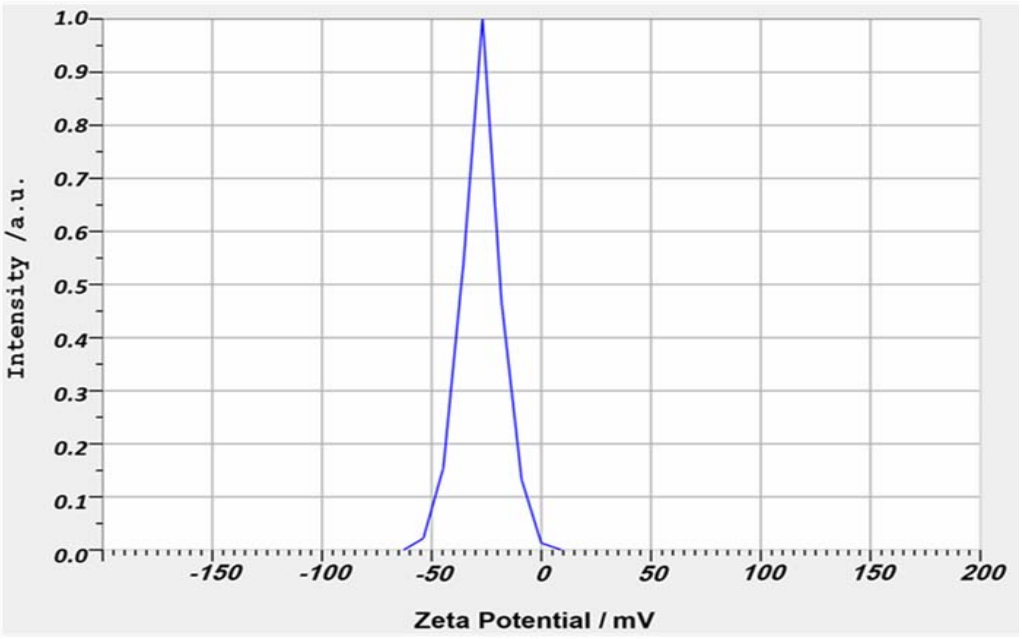

Figure 5: Zeta potential curve for aqueous solution of as-obtained NCQDs**.**

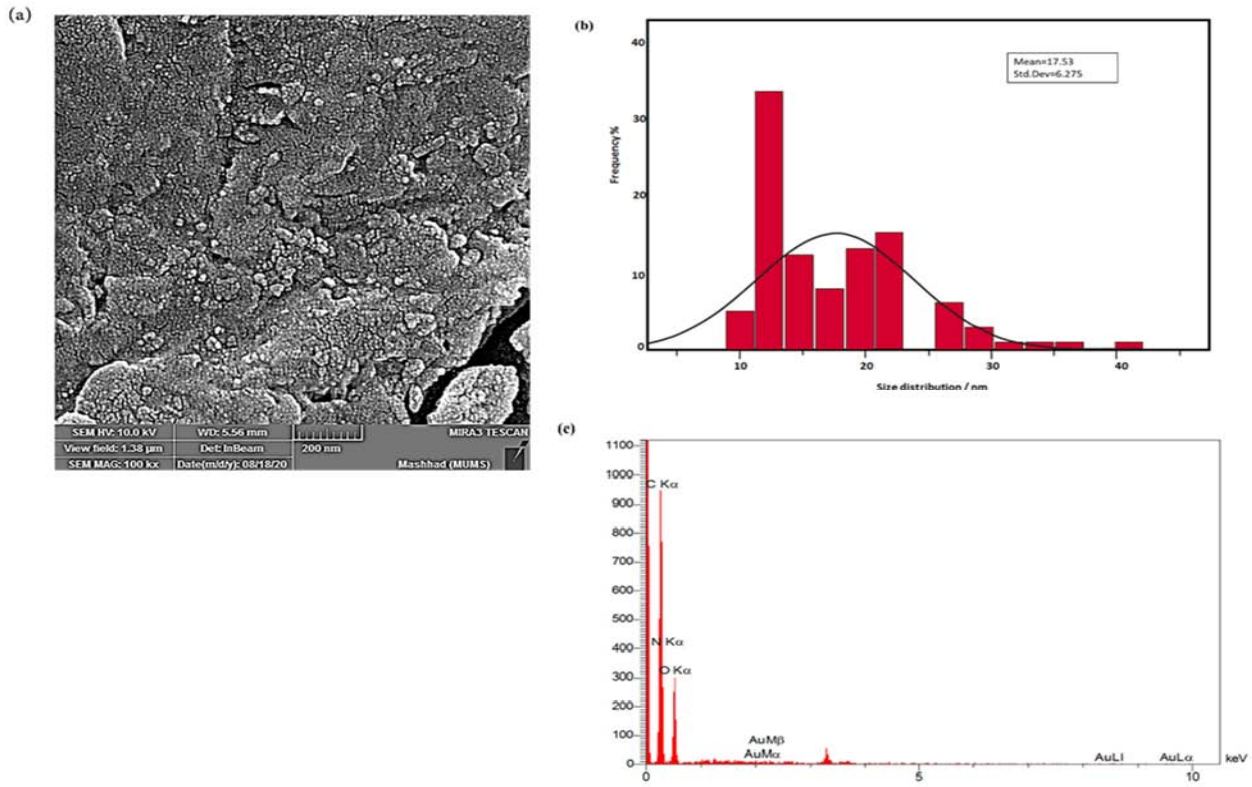

Figure 6: FESEM photograph for natural carbon quantum dots (a) scale bar 200 nm, histogram image of NCQDs with an average size of 17 nm (b). EDX spectrum of natural carbon quantum dots (c).

NCQDs as result revealed. The zeta potential value is shown in (Figure 5). A zeta potential value that had been -27.4mV which indicates the negatively charged carboxyl (-COOH) and hydroxyl (-OH) functional group on the surface of NCQDs [54].

Microscopic images: Field-scanning electron microscopy (FE-SEM) was investigated the morphology of samples and along with size distribution (Figure 6). The FE-SEM image approximately illustrated the presence of spherical shape of NCQDs (Figure 6a). The average

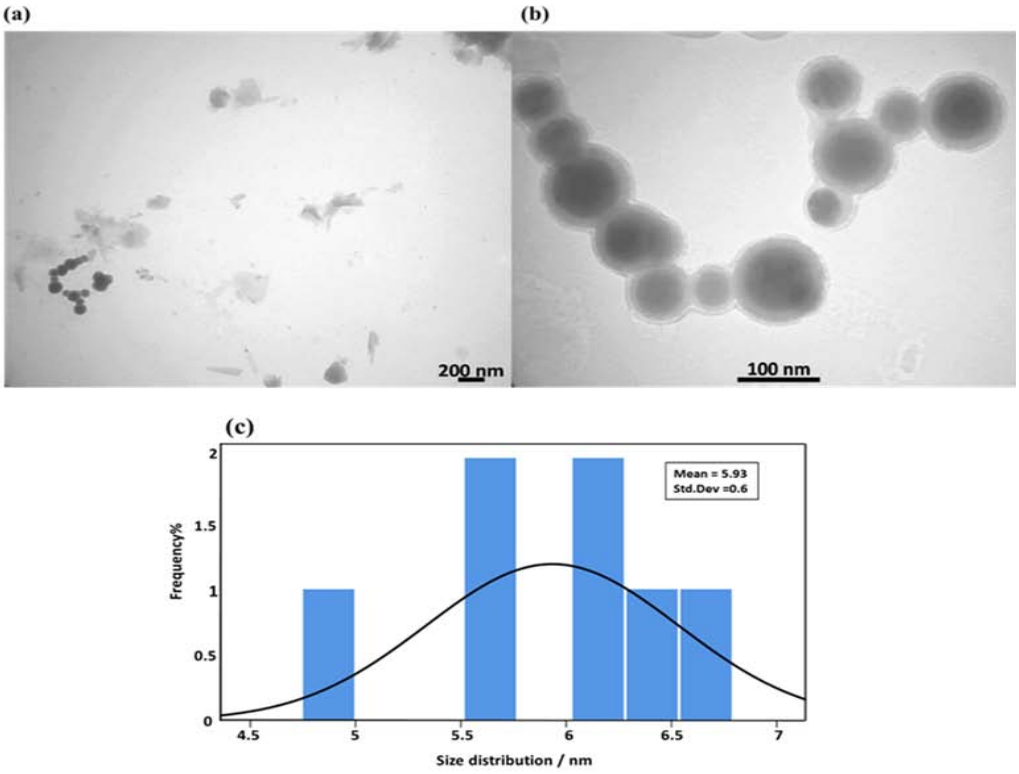

Figure 7: The transmission electron microscope images of the as- prepared NCQDs (a) scale bar indicates 200 nm, (b) shows individual spherical particle chains, scale bar indicates 100 nm, (c) demonstrated the size distribution histogram of the prepared NCQDs with the average size of 5.9 nm.

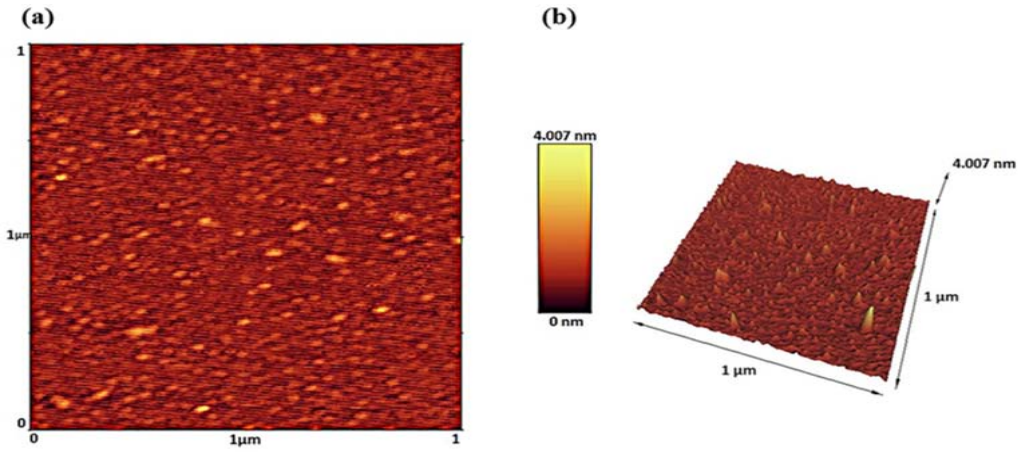

Figure 8: AFM images of the NCQDs, (a) two dimensional image of NCQDs and (b) three dimensional image of NCQDs (b).

size distribution of NCQDs was about 17 nm that demonstrated in the histogram (Figure 6b). The statistical analysis of samples dimensions based upon the FE-SEM images have been measured by using of image J software. Energy Dispersive Electron (EDX) attached with FE-SEM was used for elemental analysis of NCQDs. The EDX pattern (Figure 6c) represent the peaks of carbon, oxygen, nitrogen and sulfur with 73.04A%, 23.16 A%, 2.06 and 0.04A% respectively which confirmed NCQDs synthesis. The absence of any extra peaks in the spectrum shows the formation of pure AU oxide nano-sheets.

The information of CQDs was confirmed by TEM investigation (Figure 7). The specific small area in (Figure 7a) magnified and showed in (Figure 7b) which clearly revealed that the prepared NCQDs were mono-dispersed with the spherical morphologies. The statistical analysis of samples dimensions based upon the TEM images have been carried out through the utilization of Image J software which display in (Figure 7c). The histogram showed the average size of the obtained NCQDs was 5.9 nm.

The topographical images were utilized for measuring the size of

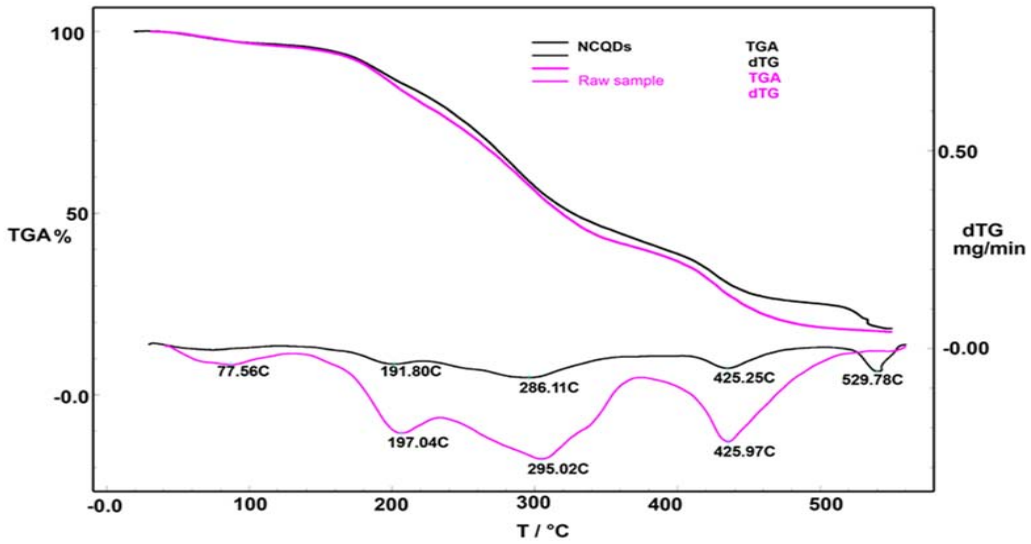

Figure 9: TGA/DTG curves of raw sample (pink lines) and the obtained NCQDs (black lines).

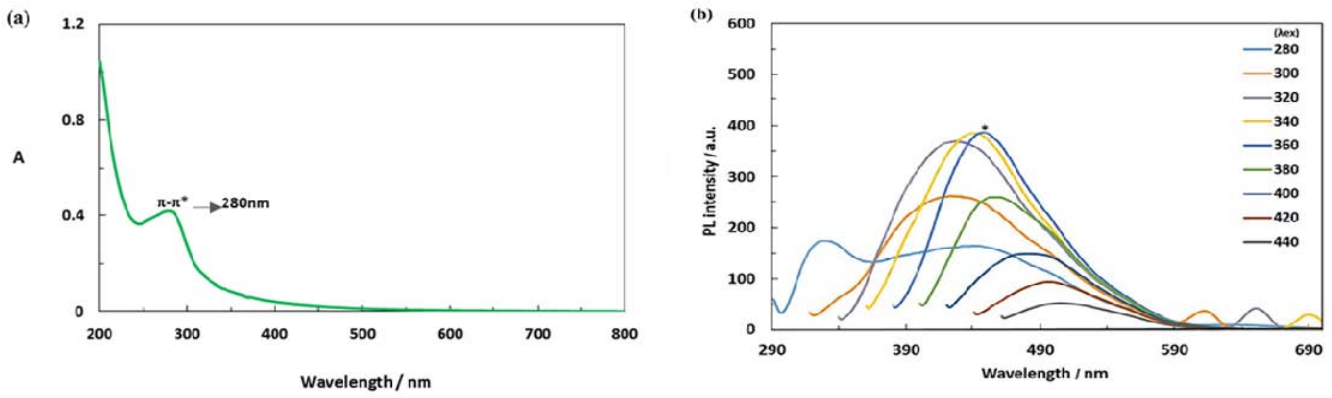

Figure 10: Optical properties of NCQDs: absorption spectra of the NCQDs in aqueous solution (λ_{ex}=280 nm) in PL emission spectra of the NCQDs in aqueous solution at different excitation wavelengths (λ_{ex}= 280 and λ_{em}= 300, 320, 340, 360, 380, 400, 420 and 440 nm) in b.

roughness of NCQDs. The two dimensional and three dimensional AFM images of NCQDs are shown in (Figure 8). It was observed that the NCQDs were found to be very small and spherical shape (Figure 8a) and the surface roughness were illustrated in (Figure 8a).

Thermogravimetric Analysis

To estimate the thermal stability and rate of weight changes of the sample (weight loss), TGA measurement of banana peel and the obtained NCQDs were performed and results are presented in (Figure 9). The first peak, below 150°C is related to absorb water which leading to approximately 5% loss of weight. The second, from 180°C to 260°C is slower which is related to 10% loss of weight, the third, from 260°C to 420°C, the weight loss is faster which leading 20% loss of weight. From 420°C to 520°C and later areas the weight less is slower and finally each elements of NCQDs decomposes at a certain temperature. It was demonstrated that the NCQDs was decompose slower than raw sample.

Optical Properties of Natural Carbon Quantum Dots

To study the optical properties of the synthesized NCQDs from banana peel, UV-visible absorption and PL-spectra was performed (Figure 10). The optical absorption peak of NCQDs aqueous solution in UV-visible region illustrated in (Figure 10a). The strong peak at about 280 nm is attributed to the π-π^*transitions of C=C sp^2 bond. According to the reports, almost all carbon dots of different luminous colors demonstrate analogous 200–350 nm absorption in UV region; these peaks are originated from the conjugate sp^2 structures in the core part of NCQDs [14,27]. (Figure 10b) indicated the PL spectra of NCQDs aqueous solution show at a different excitation with varying from 280 nm to 440 nm at intervals of 20 nm. The increasing excitation peaks demonstrate at 360 nm which show the high intensity emission appears at 384.1 nm in the obtained NCQDs and after that the intensity emission gradually decrease. Besides, The PL emission of the NCQDs is gradually red shifted, which increase in upper excitation wavelength, demonstrating the excitation-dependent property of the NCQDs.

MTT Assay

Biocompatibility and bio viability are indispensable factors that must be considered for being utilized in future medical applications.

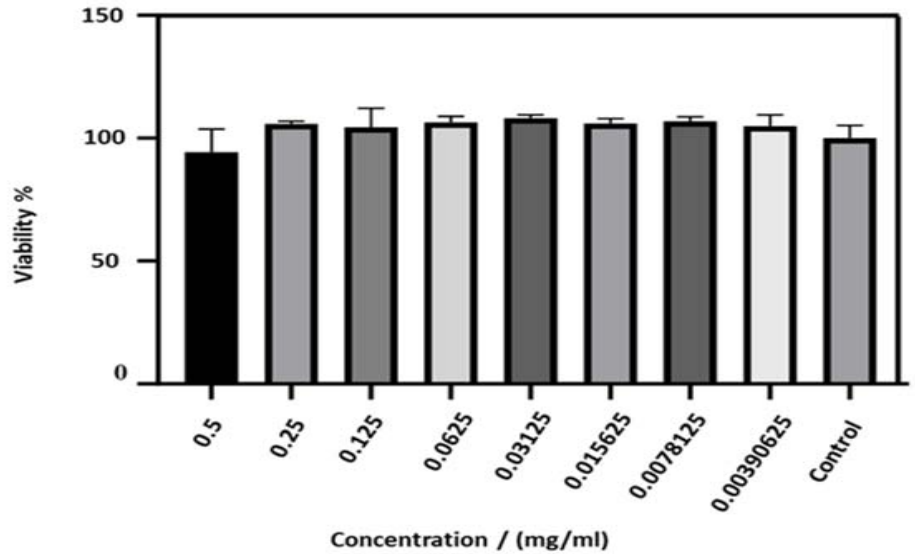

Figure 11: Cytotoxicity of NCQDs against of mouse normal fibroblast cell line increasing concentration from 0.0039 to 0.5 mg⁄ml.

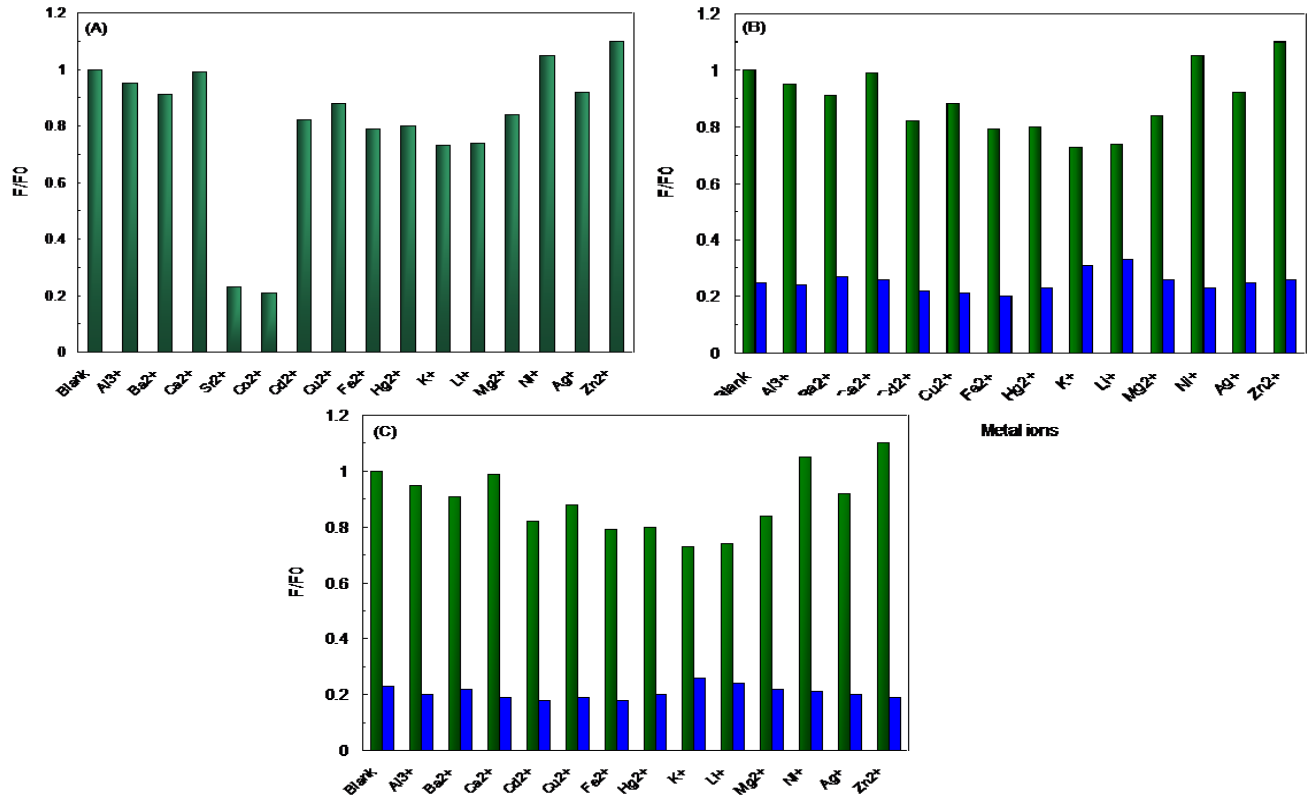

Figure 12: (A) Relative fluorescence intensity of NCQDs in the presence of various metal ions (0.1 mM). (B) Selectivity of NCQDs for Sr^{2+} coexisting with 0.1 mM of other ions; green color (without Sr^{2+}) and blue color (With Sr^{2+}). (C) Selectivity of NCQDs for Co^{2+} coexisting with 0.1 mM of other ions; green color (without Co^{2+}) and blue color (With Co^{2+}).

To examine the biocompatibility behavior of the obtained NCQDs, we studied the in vitro cytotoxicity of the samples by MTT assay. It has been confirmed by the in vitro cytotoxicity examinations that the NCQDs have not caused any cellular toxicity influences on the, mouse normal fibroblast cell line, which is represented in (Figure 11), and have verified this result in different doses (0.0039 to 0.5 mg⁄ml).

Reaction of NCQDs to Sr^{2+} and Co^{2+}

Carbon quantum dots [17,18] are most commonly exerted for ion detection and in this regard, its disappearance throughout (Figure

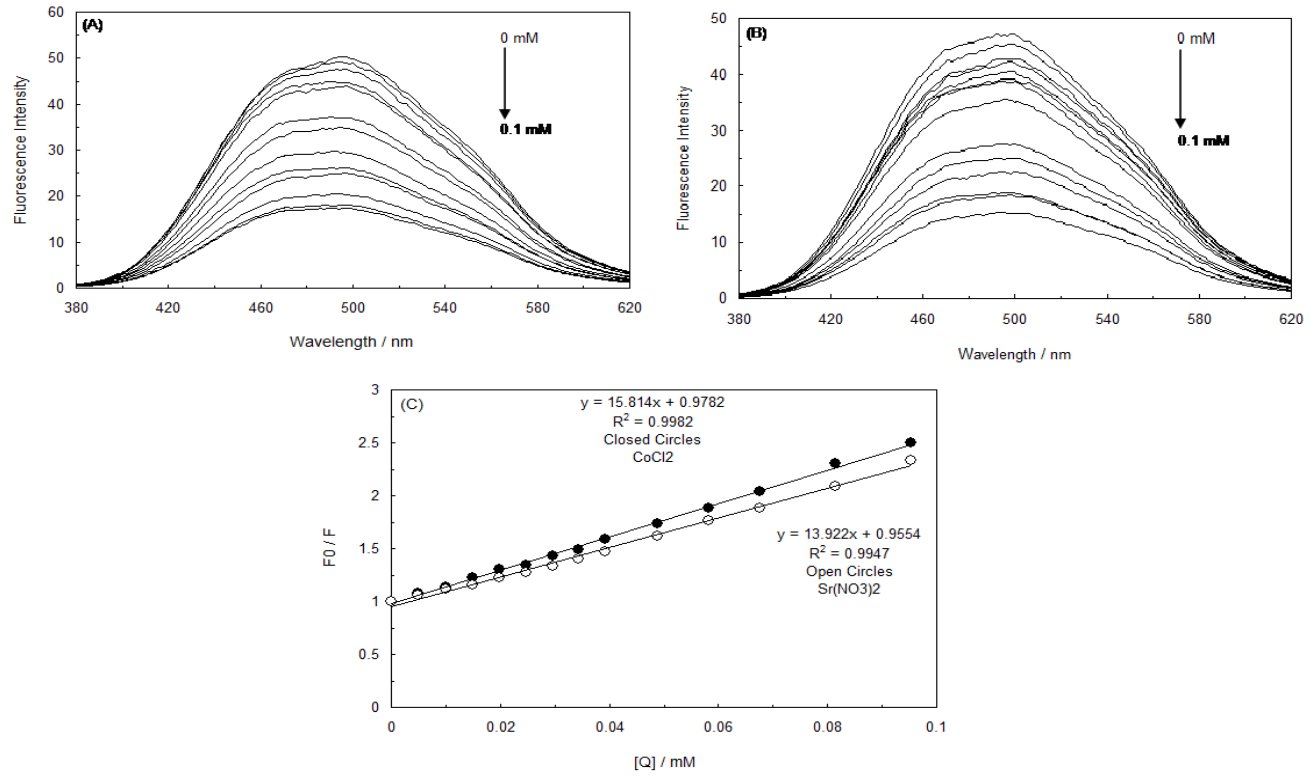

Figure 13: (A) and (B); Fluorescence emission spectra of NCQDs solution at different concentrations of Sr^{2+} and Co^{2+} respectively by 365 nm excitation wavelength. (C) Relationship between F_0/F and the concentration of Sr^{2+} (open circles) and Co^{2+} (closed circles), that reveal a linear relationship within the range of 0 – 0.1 mM.

12a) approved the effect of Sr^{2+} and Co^{2+} presence in quenching the fluorescence of NCQDs. In order to analyze the selectivity of NCQDs towards Sr^{2+} and Co^{2+}, the fluorescence intensity was evaluated in the appearance of several ions. In conformity to (Figure 12a), although Sr^{2+} and Co^{2+}caused a reduction in fluorescence intensity, yet there were no specific alterations observed throughout the F/F_0 of NCQDs subsequent to immitting 0.1 mM of other common metal ions (Al^{3+}, Ba^{2+}, Ca^{2+}, Sr^{2+}, Co^{2+}, Cd^{2+}, Cu^{2+}, Fe^{2+}, Hg^{2+}, K^{+}, Li^{+}, Mg^{2+}, Ni^{+}, Ag^{+}, Zn^{2+}). Therefore, the applicability of NCQDs in monitoring Sr^{2+} and $Co^{2+}$was indicated by the achieved outcomes.

Ncqds for the Detection of Sr^{2+} and Co^{2+}

In this section, an assessment was performed on the interference of other common ions on the quenching of Sr^{2+} and Co^{2+} to better comprehend the viability of the progressed NCQDs in practical fields. According to (Figure 12b and c), the impact of interference can be disregarded [49] upon the coexistence of other metal ions with Sr^{2+} and Co^{2+}, respectively. Thus, it can be suggested that the CQDs can exhibit a satisfying identification for the detection of Sr^{2+} and Co^{2+} in the lack of other metal ions interference.

CQDs are capable of acting in the role of fluorescent sensors for detecting the content of Sr^{2+} and Co^{2+}. (Figure 13a and b) presents the fluorescence emission spectra of NCQDs solution next to the increasing concentrations of Sr^{2+} and Co^{2+}. Subsequent to having reactions for 3 min at 25°C, the measurement of fluorescence spectra was completed under the excitation wavelength of 365nm. A gradual reduction was caused in the intensity as the concentration of Sr^{2+} and $Co^{2+}$was increased, which implicated the invariability of spectra's shape and position.

The provided Stern-Volmer equation in the following represents the relationship of the relative fluorescence intensity values and the concentrations of Sr^{2+} and Co^{2+}:

$$F_0/F = 1 + K_{sv}[Q] \quad (3)$$

In the Eq. 3, F_0 and F stand for the fluorescence intensity of NCQDs throughout the absence and attendance of the ions, respectively, [Q] represents the volume of Sr^{2+} and Co^{2+}, and K_{sv} refers to the quenching association constant.

According to the obtained fitting curves from the ratios of F_0/F and the volume of two cations, a fine linearity was achieved throughout the range of 0-0.1 mM with the correlation coefficients of 0.9955 and 0.9944 for Sr^{2+} and Co^{2+}, respectively (Figure 13c). The K_{sv} values of the binding of Sr^{2+} and Co^{2+} to NCQDs were to be 1.39 $\times 10^4$ M^{-1} and 1.58 $\times 10^4$ M^{-1} respectively that showed more binding affinity of Co^{2+} to NCQDs than to Sr^{2+} that reveal the NCQDs can be considered as a sensor with more sensitive.

Conclusions

This paper has demonstrated a new method for the synthesis of natural carbon quantum dots by the usage of banana peel. In this process of banana peel waste examining for the NCQDs synthesis, a bio-friendly and highly luminescent NCQDs synthesis is being reported, without any use of additional oxidizing agents. The

resultant NCQDs with an acceptable quantum yield of 12 % show high water stability and solubility has spherical morphology with an average 5.9 nm, exhibits an acceptable degree of graphitization and their zeta potential reached up to -27.4 mV. Further, we studied the effect of these on mouse normal fibroblast cell line by MTT assay that showed the synthesized NCQDs have low toxicity and favorable biocompatibility. These results may motivate the cost-effective, green and sustainable synthesis of highly fluorescent multifunctional carbon-based nano-materials with various future potential biological applications. The exertion of the produced NCQDs in the form of a highly sensitive and selective sensor for the detection of Sr^{2+} and Co^{2+}, which was contingent on a fluorescence on-off switch model, proved to be quiet successful. The K_{sv} values of Sr^{2+}-NCQDs and Co^{2+}-NCQDs for Co^{2+} is more sensitive than Sr^{2+}.

Acknowledgements

The financial support of the Research Council of the Mashhad Branch, Islamic Azad University is gratefully acknowledged. The authors thank Dr. Ljungburg for English editing.

Conflicts of Interest

The authors declare no conflict of interest, financial or otherwise.

References

1. Ahn JY Song, JE Kwon, SH Lee, KS Park, S Kim, et al. Food waste-driven N-doped carbon dots: Applications for Fe3+ sensing and cell imaging. Materials Science and Engineering: 2019; 102: 106-112.
2. Alam AM, BY Park, ZK Ghouri, M Park, HY Kim. Synthesis of carbon quantum dots from cabbage with down- and up-conversion photoluminescence properties: excellent imaging agent for biomedical applications. Green Chemistry 2015; 17: 3791-3797.
3. Ansi VA, NK Renuka. Table sugar derived Carbon dot – a naked eye sensor for toxic Pb2+ ions. Sensors and Actuators B: Chemical. 2018; 264: 67-75.
4. Arumugam SS, J Xuing, A Viswadevarayalu, Y Rong, D Sabarinathan, et al. Facile preparation of fluorescent carbon quantum dots from denatured sour milk and its multifunctional applications in the fluorometric determination of gold ions, in vitro bioimaging and fluorescent polymer film. Journal of Photochemistry and Photobiology A: Chemistry. 2020; 401: 112788.
5. Atchudan R, TNJI Edison, S Perumal, N Clament Sagaya Selvam, YR Lee. Green synthesized multiple fluorescent nitrogen-doped carbon quantum dots as an efficient label-free optical nanoprobe for in vivo live-cell imaging. Journal of Photochemistry and Photobiology A: Chemistry. 2019; 372: 99-107.
6. Atchudan R, TN Jebakumar Immanuel Edison, M Shanmugam, S Perumal, T Somanathan. et al. Sustainable synthesis of carbon quantum dots from banana peel waste using hydrothermal process for in vivo bioimaging. Physica E: Low-dimensional Systems and Nanostructures. 2021; 126: 114417.
7. Baig MMF, YC Chen. Bright carbon dots as fluorescence sensing agents for bacteria and curcumin. Journal of Colloid and Interface Science. 2017; 501: 341-349.
8. Bhunia SK, A Saha, AR Maity, SC Ray, NR Jana. Carbon Nanoparticle-based Fluorescent Bioimaging Probes. Scientific Reports. 2013; 3: 1473.
9. Chandra S, TK Mahto, AR Chowdhuri, B Das, Sk Sahu. One step synthesis of functionalized carbon dots for the ultrasensitive detection of Escherichia coli and iron (III). Sensors and Actuators B: Chemical. 2017; 245: 835-844.
10. Cui L, X Ren, J Wang, M Sun. Synthesis of homogeneous carbon quantum dots by ultrafast dual-beam pulsed laser ablation for bioimaging. Materials Today Nano. 2020; 12: 100091.
11. Cutrim ESM, AAM Vale, D Manzani, HS Barud, E Rodríguez-Castellón, et al. Preparation, characterization and in vitro anticancer performance of nanoconjugate based on carbon quantum dots and 5-Fluorouracil. Materials Science and Engineering: C: 2020; 120: 111781.
12. Das P, S Ganguly, T Agarwal, P Maity, S Ghosh, et al. Heteroatom doped blue luminescent carbon dots as a nano-probe for targeted cell labeling and anticancer drug delivery vehicle. Materials Chemistry and Physics. 2019; 237: 121860.
13. Devi S, RK Gupta, AK Paul, S Tyagi. Waste carbon paper derivatized Carbon Quantum Dots/(3-Aminopropyl)triethoxysilane based fluorescent probe for trinitrotoluene detection. Materials Research Express. 2018; 6: 025605.
14. Ding H, SB Yu, JS Wei, HM Xiong. Full-Color Light-Emitting Carbon Dots with a Surface-State-Controlled Luminescence Mechanism. ACS Nano. 2016; 10: 484-491.
15. Dong G, K Lang, H Ouyang, W Zhang, L Bai, et al. Facile synthesis of N, P-doped carbon dots from maize starch via a solvothermal approach for the highly sensitive detection of Fe3+. RSC Advances. 2020; 10: 33483-33489.
16. Freeman R, I Willner. Optical molecular sensing with semiconductor quantum dots (QDs). Chem Soc Rev. 2012; 41: 4067-4085.
17. Gao X, C Du, Z Zhuang, W Chen. Carbon quantum dot-based nanoprobes for metal ion detection. Journal of Materials Chemistry C. 2016; 4: 6927-6945.
18. Guo Y, L Zhang, S Zhang, Y Yang, X Chen, et al. Fluorescent carbon nanoparticles for the fluorescent detection of metal ions." Biosensors and bioelectronics. 2015; 63: 61-71.
19. Gupta DA, ML Desai, NI Malek, SK Kailasa. Fluorescence detection of Fe3+ ion using ultra-small fluorescent carbon dots derived from pineapple (Ananas comosus): Development of miniaturized analytical method. Journal of Molecular Structure. 2020; 1216: 128343.
20. He D, C Zheng, Q Wang, C He, YI Lee, et al. Dielectric barrier discharge-assisted one-pot synthesis of carbon quantum dots as fluorescent probes for selective and sensitive detection of hydrogen peroxide and glucose. Talanta. 2015; 142: 51-56.
21. Hu X, Y Li, Y Xu, Z Gan, X Zou, et al. Green one-step synthesis of carbon quantum dots from orange peel for fluorescent detection of Escherichia coli in milk. Food Chemistry. 2021; 339: 127775.
22. Huang C, X Wang, C Liang, X Jiang, G Yang, et al. A sustainable process for procuring biologically active fractions of high-purity xylooligosaccharides and water-soluble lignin from Moso bamboo prehydrolyzate. Biotechnology for Biofuels. 2019; 12: 189.
23. Huo F, Z Kang, M Zhu, C Tan, Y Tang, et al. Metal-triggered fluorescence enhancement of multicolor carbon dots in sensing and bioimaging. Optical Materials. 2019; 94: 363-370.
24. Huo X, Y He, S Ma, Y Jia, J Yu, et al. Green Synthesis of Carbon Dots from Grapefruit and Its Fluorescence Enhancement. Journal of Nanomaterials. 2020; 2020: 8601307.
25. Jing S, Y Zhao, RC Sun, L Zhong, X Peng. Facile and High-Yield Synthesis of Carbon Quantum Dots from Biomass-Derived Carbons at Mild Condition. ACS Sustainable Chemistry & Engineering. 2019; 7: 7833-7843.
26. Kairdolf BA, AM Smith, TH Stokes, MD Wang, AN Young, et al. Semiconductor Quantum Dots for Bioimaging and Biodiagnostic Applications. Annual Review of Analytical Chemistry. 2013; 6: 143-162.
27. Li J, T Lu, Z Zhao, R Xu, Y Li, et al. Preparation of heterostructured ternary Cd/CdS/BiOCl photocatalysts for enhanced visible-light photocatalytic degradation of organic pollutants in wastewater. Inorganic Chemistry Communications. 2020; 121: 108236.
28. Li N, F Lei, D Xu, Y Li, J Liuet al. One-step synthesis of N, P Co-doped orange carbon quantum dots with novel optical properties for bio-imaging. Optical Materials. 2021; 111: 110618.
29. Liu X, J Hao, J Liu, H Tao. Green synthesis of carbon quantum dots from lignite coal and the application in Fe3+detection. IOP Conference Series: Earth and Environmental Science. 2018; 113: 012063.
30. Lu M, Y Duan, Y Song, J Tan, L Zhou. Green preparation of versatile nitrogen-doped carbon quantum dots from watermelon juice for cell imaging, detection

of Fe3+ ions and cysteine, and optical thermometry. Journal of Molecular Liquids. 2018; 269: 766-774.

31. Madhu M, TH Chen, WL Tseng. White-light emission of single carbon dots prepared by hydrothermal carbonization of poly(diallyldimethylammonium chloride): Applications to fabrication of white-light-emitting films. Journal of Colloid and Interface Science. 2019; 556: 120-127.

32. Mary Alex A, MD Kiran, G Hari, A Krishnan, JS Jayan, et al. Carbon dots: A green synthesis from Lawsonia inermis leaves. Materials Today: Proceedings. 2020; 26: 716-719.

33. Meena R, R Singh, G Marappan, G Kushwaha, N Gupta, et al. Fluorescent carbon dots driven from ayurvedic medicinal plants for cancer cell imaging and phototherapy. Heliyon. 2019; 5: e02483.

34. Mehta VN, S Jha, SK Kailasa. One-pot green synthesis of carbon dots by using Saccharum officinarum juice for fluorescent imaging of bacteria (Escherichia coli) and yeast (Saccharomyces cerevisiae) cells. Materials Science and Engineering: C. 2014; 38: 20-27.

35. Pajewska-Szmyt M, B Buszewski, R Gadzała-Kopciuch. Sulphur and nitrogen doped carbon dots synthesis by microwave assisted method as quantitative analytical nano-tool for mercury ion sensing. Materials Chemistry and Physics. 2020; 242: 122484.

36. Park SY, CY Lee, HR An, H Kim, YC Lee, et al. Advanced carbon dots via plasma-induced surface functionalization for fluorescent and bio-medical applications. Nanoscale. 2017; 9: 9210-9217.

37. Puvvada N, BNP Kumar, S Konar, H Kalita, M Mandal. Synthesis of biocompatible multicolor luminescent carbon dots for bioimaging applications. Science and Technology of Advanced Materials. 2012; 13: 045008.

38. Qiang R, S Yang, K Hou, J Wang. Synthesis of carbon quantum dots with green luminescence from potato starch. New Journal of Chemistry. 2019; 43: 10826-10833.

39. S Thambiraj, DR Shankaran. Green synthesi s of highly fluorescent carbon quantum dots from sugarcane bagasse pulp. Applied Surface Science. 2016; 390: 435-443.

40. Shukla D, M Das, D Kasade, M Pandey, AK Dubey, et al. Sandalwood-derived carbon quantum dots as bioimaging tools to investigate the toxicological effects of malachite green in model organisms. Chemosphere. 2020; 248: 125998.

41. Singh H, A Bamrah, M Khatri, N Bhardwaj. One-pot hydrothermal synthesis and characterization of carbon quantum dots (CQDs). Materials Today: Proceedings. 2020; 28: 1891-1894.

42. Singh L, T Sharma, V Singh. Study of structural and functional properties of fluorescent EDTA@CQDs synthesized from peanut shells via pyrolysis technique. Materials Today: Proceedings. 2021; 44: 192-198.

43. Sun R, S Liu. Synthesis of photoluminescent carbon dots and its effect on chondrocytes for knee joint therapy applications. Artificial Cells, Nanomedicine, and Biotechnology. 2019; 47: 1321-1325.

44. Thulasi S, A Kathiravan, M Asha Jhonsi. Fluorescent Carbon Dots Derived from Vehicle Exhaust Soot and Sensing of Tartrazine in Soft Drinks. ACS Omega. 2020; 5: 7025-7031.

45. V Roshini, S Misra, MK Santra, D Ottoor. One pot green synthesis of C-dots from groundnuts and its application as Cr(VI) sensor and in vitro bioimaging agent. Journal of Photochemistry and Photobiology A: Chemistry. 2019; 373: 28-36.

46. Vairavapandian D, P Vichchulada, MD Lay. Preparation and modification of carbon nanotubes: Review of recent advances and applications in catalysis and sensing. Analytica Chimica Acta. 2008; 626: 119-129.

47. Wang C, H Shi, M Yang, Y Yan, E Liu, et al. Facile synthesis of novel carbon quantum dots from biomass waste for highly sensitive detection of iron ions. Materials Research Bulletin. 2020; 124: 110730.

48. Wang M, H Yin, Y Zhou, X Meng, GIN Waterhouse, et al. A novel photoelectrochemical biosensor for the sensitive detection of dual microRNAs using molybdenum carbide nanotubes as nanocarriers and energy transfer between CQDs and AuNPs. Chemical Engineering Journal. 2019; 365: 351-357.

49. Wang X, X Yang, N Wang, J Lv, H Wang, et al. Graphitic carbon nitride quantum dots as an “off-on” fluorescent switch for determination of mercury (II) and sulfide. Microchimica Acta. 2018; 185: 1-8.

50. Wongso V, HK Chung, NS Sambudi, S Sufian, B Abdullah, et al. Silica–carbon quantum dots decorated titanium dioxide as sunlight-driven photocatalyst to diminish acetaminophen from aquatic environment. Journal of Photochemistry and Photobiology A: Chemistry. 2020; 394: 112436.

51. Xu X, R Ray, Y Gu, HJ Ploehn, L Gearheart, et al. Electrophoretic Analysis and Purification of Fluorescent Single-Walled Carbon Nanotube Fragments. Journal of the American Chemical Society. 2004; 126: 12736-12737.

52. Xu Z, J Liu, K Wang, B Yan, S Hu, et al. Facile synthesis of N-doped carbon dots for direct/indirect detection of heavy metal ions and cell imaging. Environmental Science and Pollution Research. 2021; 28: 19878-19889.

53. Zavareh HS, M Pourmadadi, A Moradi, F Yazdian, M Omidi. Chitosan/carbon quantum dot/aptamer complex as a potential anticancer drug delivery system towards the release of 5-fluorouracil. International Journal of Biological Macromolecules. 2020; 165: 1422-1430.

54. Zulfajri M, S Dayalan, WY Li, CJ Chang, YP Changet al. Nitrogen-Doped Carbon Dots from Averrhoa carambola Fruit Extract as a Fluorescent Probe for Methyl Orange. Sensors (Basel). 2019; 19: 5008.